FISFVIFR

Contents lists available at SciVerse ScienceDirect

Microelectronics Reliability

journal homepage: www.elsevier.com/locate/microrel



Effects of single vacancy defect position on the stability of carbon nanotubes

R.H. Poelma a,*, H. Sadeghian , S. Koh , G.Q. Zhang a,b

ARTICLE INFO

Article history: Received 2 October 2011 Received in revised form 30 January 2012 Accepted 6 March 2012 Available online 26 April 2012

ABSTRACT

In this paper, the buckling behavior of fixed-fixed, both single- and multi- wall carbon nanotubes (CNTs) under axial compressive loads, are studied using analytical continuum theory and molecular dynamics (MD). An approach based on the tethering of atoms (applying a spring force), is used to apply the boundary conditions and extract the reaction forces during the MD simulation. The effects of the vacancy defect position on the CNT critical buckling load are studied at room temperature and at low temperature (1 K). It is concluded that the defects at the ends of the CNT and close to the middle of the CNT significantly reduce the critical buckling load and strain of CNTs at 1 K. At room temperature the influence of vacancy defects on the critical buckling load and strain appears to be small. The MD simulation results can prove to be useful for developing more accurate continuum descriptions of the CNT mechanics in future research.

© 2012 Elsevier Ltd. All rights reserved.

1. Introduction

Carbon nanotubes (CNTs) are attracting much interest due to their exceptional mechanical, thermal and electrical properties. Many promising applications have been suggested for CNTs ranging from: sensing, imaging, energy storage and interconnect technology to fiber reinforced materials [1]. Recent examples of technologies that contain CNTs are nano-interconnects [2–4], nano- electro mechanical systems (NEMS) [5], nanocomposites [6–9] and atomic force microscope (AFM) tips [6,10,11].

The mechanical behavior of CNTs has been the subject of many experimental, molecular dynamics (MD), and elastic continuum modeling studies [12,13]. Because of their high aspect ratio, CNTs may easily become mechanically unstable and buckle under compressive axial loads [6]. Buckling is a mechanical instability which can lead to failure in the form of a sudden reduction of the load carrying capability of the structure, an undesirable distorted configuration or electrical shortcuts. Therefore, particular interest has been shown in the mechanical stability of CNTs that are used in nanocomposites and AFM tips [6,7,14]. However, experimental studies on the mechanical behavior of small structures becomes challenging at the nanoscale due to the increased difficulty in handling, specimen fabrication, deformation detection and force loading [15]. Recently, novel experimental approaches have been introduced for accurate and robust measurement of material properties at the nanoscale [16,17].

In order to overcome limitations of experiments, computational methods are used for studying the parameters that influence the mechanical stability of CNTs. In addition, more realistic models are needed to predict and understand the mechanical behavior of CNTs and other materials in experiments and applications better [18]. One approach is to include vacancy defects (missing atoms) into the atomistic model of the CNT. The vacancy defects can be formed during the CNT synthesis or they can be formed under high temperature environments or stress [12,19]. Therefore several theoretical studies on CNTs have already considered the effects of vacancy defects on the elastic properties [20], the fracture strength [21] and the critical buckling load [12,19,22]. It has been mentioned that single vacancy defects have a weak effect on the critical buckling load of slender (length/diameter ≥ 12) CNTs at room temperature [22]. However, most of these studies considered defect locations at the middle of the axial compressive loaded CNTs. The aim of this study is to explore the effects of the position of the single vacancy defects on the CNT critical buckling load at low temperature and room temperature by performing MD simulations. Furthermore, the CNT Euler modes were determined by comparing the MD simulation results with the continuum theory of Euler buckling for different CNT geometrical dimensions.

2. Theory: molecular dynamics

Molecular dynamics has become an important tool for studying the properties of materials and structures [23]. Molecular dynamics is a computer simulation technique where the equations of motion of atoms and molecules are solved numerically over time. The modeled particles are allowed to interact with each-other by

^a Department of Microelectronics, Delft University of Technology, Feldmannweg 17, 2628 CT Delft, The Netherlands

^b Philips Lighting, Mathildelaan 1, 5611 BD Eindhoven, The Netherlands

^{*} Corresponding author. Tel.: +31 (0) 15 27 82311. E-mail address: R.H.Poelma@tudelft.nl (R.H. Poelma).

means of forcefields [24]. MD simulations can provide details, or control individual particle motion, more easily than experiments on a similar system [25]. Therefore, we choose MD to study the effects of the position of missing atoms (vacancy defects) on the mechanical stability of CNTs.

In our study, we numerically calculate the load–displacement curve of defective and non-defective CNTs under uniaxial compression and determine the buckling load. Modeling of CNTs was carried out with the commercial computational materials program *Material Studio 5.0* and the module *Forcite* from Accelrys [26]. The scripts were developed with the programming language *Perl*.

2.1. Dreiding forcefield

The generic *Dreiding* forcefield is used to regulate the bonded and non-bonded interaction forces between the carbon atoms during the simulation [24]. The atomistic interaction forces can be described using the potential energy that is required for the different types of bond deformation, see respectively Fig. 1a–d. The function that describes the total potential energy of the system is expressed as.

$$E_{P} = \sum_{bonds} E_{r} + \sum_{anales} E_{\theta} + \sum_{dihedrals} E_{\phi} + \sum_{inversion} E_{\omega} + \sum_{nonbond} E_{nb}$$
 (1)

where E_r , E_θ , E_ϕ , E_ω and E_{nb} are respectively the bond stretching energy, angle bending energy, torsional energy, inversion energy and the non-bond energy [24,27].

$$E_r = \frac{1}{2}k_r(r - r_0)^2 \tag{2}$$

The stretching energy is given by Eq. (2), the equilibrium bond length and bond stiffness between the atoms i and j in Fig. 1a, are denoted by respectively r_0 and k_r . The energy terms given by Eqs. (3)–(6), refer to the angle bending and torsion terms,

$$E_{\theta} = \frac{1}{2}k_{\theta}(\theta - \theta_0)^2 \tag{3}$$

$$E_{\phi} = \frac{1}{2}k_{\phi}(1 - \cos[2(\phi - \phi_0)]). \tag{4}$$

For out of plane-equilibrium inversion angles: $\omega_0 \neq 0$, Eq. (5) is used,

$$E_{\omega} = \frac{1}{2} k_{\omega} ((\cos \omega - \cos \omega_0) / \sin \omega_0)^2. \tag{5}$$

For in-plane configurations ω_0 = 0, Eq. (6) is used,

$$E_{\omega} = \frac{1}{2}k_{\omega}(1 - \cos\omega)^2. \tag{6}$$

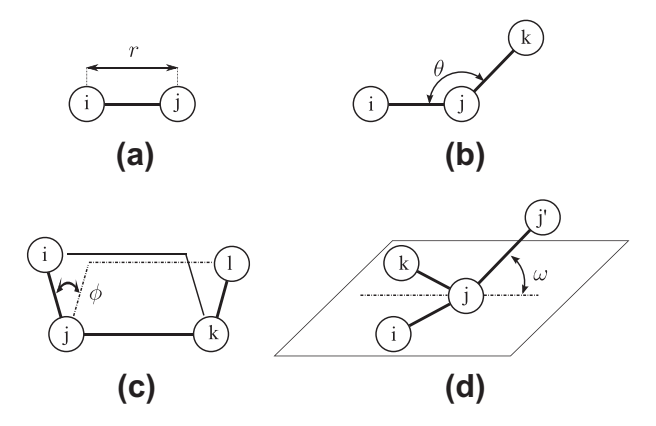


Fig. 1. Schematic illustration of the different Dreiding functional terms that describe the bonded interaction between the atoms: (a) bond stretch, (b) angle bend, (c) torsion, (d) inversion.

The bonded constants, k_{θ} , k_{ϕ} , r_0 , θ_0 , etc. can be found elsewhere for a variety of different atomistic interactions [24]. The non-bonded interactions, such as van der Waals (vdW) and electrostatic (Coulomb) are given by

$$E_{IJ} = D_0 \left[\left(\frac{r_0}{r} \right)^{12} - 2 \left(\frac{r_0}{r} \right)^{6} \right]. \tag{7}$$

$$E_C = C \frac{q_i q_j}{\varepsilon r}. ag{8}$$

For the vdW interaction, constant D_0 can be found in [24]. The electrostatic interactions are calculated by using Eq. (8), where q_i and q_j are the respective charges of the particles, r the distance and ϵ the dielectric constant [24,26]. The sum of the E_{Lj} and E_C forms E_{nb} , which is the total non-bonded potential energy. Recent MD studies have shown that the *Dreiding* forcefield can be successfully used for the predictions of the elastic properties of CNT composites, yield criterion for PMMA and the crystallization of polymer chains on the CNT walls, respectively [18,27,28]. Furthermore, the *Dreiding* forcefield parameters can be extended to include atomic bonds with a user specified stiffness and length.

2.2. Boundary conditions and reaction forces

Fig. 2 shows a schematic representation of a single wall CNT with applied boundary conditions. The ends of the CNT are fixed to linear elastic tethers (springs). The tethers have a user specified stiffness k and reference length l_0 . The tethers are fixed between the atoms at the ends of the CNT and the anchor points. The anchor points have fixed translational degrees of freedom in a Cartesian reference frame. When the anchor points at one boundary are given a small incremental displacement, the tethers are stretched and a restoring force is created within the tethers. The tether stiffness is high compared to the stiffness of the atomistic bonds and is used in the calculation of the reaction force.

The restoring spring force is determined by the multiplication of the tether stiffness k with the tether elongation

$$f^{i} = k \left(l^{i} - l_{0}^{i} \right), \tag{9}$$

where i is the index number of the boundary atom, l^i is the current tether length after applying the displacement and l^i_0 is the reference tether length. The reference (undeformed) tether length is determined after the equilibration of the CNT to a specified temperature and before any prescribed displacement. The current tether length is the norm of \mathbf{B} , which is the distance vector between the anchor point coordinates $\mathbf{x}_{\mathbf{p}}$ and the boundary atom coordinates $\mathbf{x}_{\mathbf{a}}$ during the MD simulation

$$l^i = \|\boldsymbol{B}^i\| = \|\boldsymbol{x}_a^i - \boldsymbol{x}_n^i\|. \tag{10}$$

The restoring force always acts in the direction of the tether. The reaction forces in x-, y- and z- direction are found by projecting the force vector onto the Cartesian axis

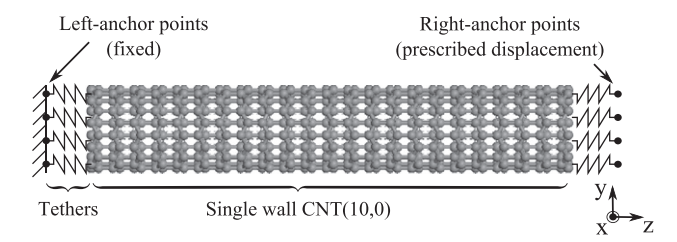


Fig. 2. Schematic illustration of a single-wall (SW) CNT and the approach used for prescribing the boundary conditions and extracting the reaction forces during the simulations

Download English Version:

https://daneshyari.com/en/article/547055

Download Persian Version:

https://daneshyari.com/article/547055

<u>Daneshyari.com</u>